

14. B. Doray, K. Bruns, P. Ghosh, S. Kornfeld, *Proc. Natl. Acad. Sci. U.S.A.* **99**, 8072 (2002).
15. S. Meresse, T. Ludwig, R. Frank, B. Hoflack, *J. Biol. Chem.* **265**, 18833 (1990).
16. L. Wan et al., *Cell* **94**, 205 (1998).
17. W. Hao, Z. Luo, L. Zheng, K. Prasad, E. M. Lafer, *J. Biol. Chem.* **274**, 22785 (1999).
18. A. Benmerah et al., *J. Cell Biol.* **140**, 1055 (1998).
19. S. A. Laporte, R. H. Oakley, J. A. Holt, L. S. Barak, M. G. Caron, *J. Biol. Chem.* **275**, 23120 (2000).
20. S. K. Mishra et al., *J. Biol. Chem.* **276**, 46230 (2001).
21. S. K. Mishra et al., *EMBO J.*, in press.
22. B. Doray, S. Kornfeld, *Mol. Biol. Cell* **12**, 1925 (2001).
23. L. H. Wang, T. C. Südhof, R. G. Anderson, *J. Biol. Chem.* **270**, 10079 (1995).
24. Mouse L cells (L5S) stably expressing GGA2-hemagglutinin (HA) were grown in α -minimum essential medium (MEM) with 10% fetal bovine serum (FBS), and HeLa cells stably expressing myc-GGA1 were maintained in Dulbecco's minimum essential medium (DMEM) with 10% FBS. They were treated with 5 mM sodium butyrate for 8 hours before fixation for immuno-electron microscopy. The wild-type and D158A mutant bovine CI-MPR were expressed in receptor-negative mouse D9 cells (10).
25. H. J. Geuze, J. W. Slot, P. A. van der Ley, R. C. T. Scheffer, *J. Cell Biol.* **89**, 653 (1981).
26. G. Raposo, M. J. Kleijmeer, G. Posthuma, J. W. Slot, H. J. Geuze, in *Weir's Handbook of Experimental Immunology*, L. A. Herzenberg, D. M. Weir, L. A. Herzenberg, C. Blackwell, Eds. (Blackwell Science, Malden, MA, ed. 5, 1997), pp. 208.1–208.11.
27. GST fusions of γ -adaplin ear (residues 703 to 822) and γ -adaplin hinge (residues 595 to 683) were expressed and purified as described (22). GST-GGA2 ear (residues 473 to 613) was prepared as reported (4). The construct encoding murine GST-AP-2- α ear (residues 701 to 938) was provided by R. G. W.

- Anderson (23). For the in vitro phosphorylation assays, GST fusion peptides of GGA1 hinge (residues 342 to 367, inclusive of the sequence Ser³⁵⁵-Leu-Leu-Asp³⁵⁸) and the cytoplasmic tail of the bovine CI-MPR were expressed and purified as described (14). The mutagenesis of the GST-GGA1 peptide fusion (S355A, D358A) was performed using primers incorporating the desired mutations with the Quick-Change system.
28. Y. Zhu, L. M. Traub, S. Kornfeld, *Mol. Biol. Cell* **9**, 1323 (1998).
29. Affinity-purified rabbit polyclonal antibody to CI-MPR was obtained from W. Gregory.
30. We thank H. Bai for the construct His-myc-GGA1 and L. Traub, D. Ory, K. Kornfeld, and R. Kornfeld for critical reading of the manuscript. Supported in part by NIH grant RO1 CA-08759 to S.K.

21 June 2002; accepted 29 July 2002

Inhibition of Retroviral RNA Production by ZAP, a CCCH-Type Zinc Finger Protein

Guangxia Gao,^{1,2} Xuemin Guo,² Stephen P. Goff^{1*}

Cells have evolved multiple mechanisms to inhibit viral replication. To identify previously unknown antiviral activities, we screened mammalian complementary DNA (cDNA) libraries for genes that prevent infection by a genetically marked retrovirus. Virus-resistant cells were selected from pools of transduced clones, and an active antiviral cDNA was recovered. The gene encodes a CCCH-type zinc finger protein designated ZAP. Expression of the gene caused a profound and specific loss of viral messenger RNAs (mRNAs) from the cytoplasm without affecting the levels of nuclear mRNAs. The finding suggests the existence of a previously unknown machinery for the inhibition of virus replication, targeting a step in viral gene expression.

Vertebrate cells have evolved many defense mechanisms to prevent or inhibit viral replication after an infection (1). A remarkable array of such antiviral proteins is induced by interferon (2), including a double-stranded RNA-dependent protein kinase (PKR) that phosphorylates eIF-2 α and inhibits translation (3); the Mx proteins, which are guanosine triphosphatases that block viral gene expression (4); and oligoA synthetases (5, 6) that activate ribonuclease (RNase) L to degrade mRNAs and ribosomal RNAs (rRNAs). In some cases, the antiviral state involves a drastic shutoff of host functions; in other cases, there is a more selective block of viral replication or gene expression. Although many parallel pathways have been uncovered, it is likely that more antiviral proteins remain to be found (7).

To identify previously unknown antiviral

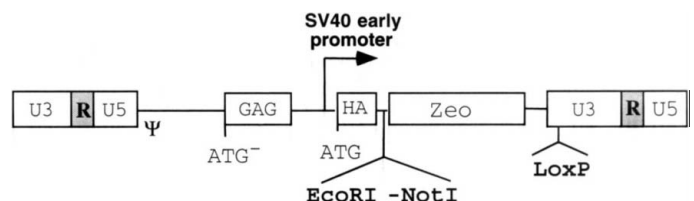
proteins, we conducted a directed search for genes that would block infection by a genetically marked retroviral genome. A library of expressed cDNAs was constructed in a retroviral vector, termed pBabe-HAZ, with several key features (Fig. 1A). Randomly primed cDNAs from wild-type Rat2 fibroblasts were inserted into the vector under the control of the constitutive SV40 early gene promoter, with a hemagglutinin (HA) epitope tag fused at their 5' ends and a Zeocin resistance gene at their 3' ends (8). A LoxP sequence, recognized by the Cre recombinase, was inserted into the U3 region of the 3' long terminal repeat (LTR). During reverse transcription of the vector, this region becomes duplicated, generating LoxP sites in both LTRs of the

integrated provirus and so allowing efficient excision of the provirus from the genome by the Cre recombinase. The complexity of the library was 2×10^7 , with inserts ranging from 0.2 to 3.5 kb.

A strategy was developed to select and recover antiviral genes in the library (8) (fig. S1). Aliquots of the library DNAs were used to transform 293T cells, along with DNAs encoding the Moloney MuLV Gag-Pol and VSV G envelope proteins, producing 20 pools of transducing viruses. These pools collectively carry most of the expressed genes of Rat2 cells. The transducing viruses were used to infect thymidine kinase-negative (TK⁻) Rat2 cells, and recipient clones were selected by culture in zeocin. Thus, each clone in the pooled cells overexpressed a single member of the cDNA library.

To identify genes in the pooled cells that conferred retrovirus resistance, we used a powerful selection for virus-resistant cells (9) (fig. S2). The pools of transduced TK⁻ Rat2 cells were challenged by repeated infection with both ecotropic and amphotropic retroviruses expressing the TK gene driven by the viral promoter, so as to transduce as many of the susceptible cells as possible. Most of the virus-sensitive cells, having now become TK-positive, were then killed by growth in the toxic thymidine analogue trifluorothymidine (TFT), and the rare TK-negative clones were recovered as candidate virus-resistant cells. Out of 5×10^5 transduced lines put through the selection, 200 TFT-resistant clones were isolated. Restesting showed that one line, L1D3, was dramatically resistant to

Fig. 1. Schematic representation of the pBabe-HAZ construct. Ψ , MuLV viral RNA packaging signal; EcoRI-Not I, linker sequence containing EcoRI and Not I sites; LoxP, LoxP sequence for recognition by Cre recombinase.



¹Howard Hughes Medical Institute, Department of Biochemistry and Molecular Biophysics, Columbia University, College of Physicians and Surgeons, 701 West 168th Street, New York, NY 10032, USA. ²Institute of Microbiology, Chinese Academy of Sciences, Beijing 100080, China.

*To whom correspondence should be addressed. E-mail: goff@cancercenter.columbia.edu

REPORTS

virus transduction. L1D3 cells were 30 times less sensitive than the parent cells to viruses carrying a luciferase reporter (an Eco-Luc virus).

To confirm that the cDNA insert in the L1D3 line was responsible for the resistance, the cells were transfected with a construct expressing the Cre recombinase (10) to induce the excision of the provirus at the LoxP sites and thereby the loss of the cDNA. Five stable transfectants were analyzed for resistance to infection by Eco-Luc virus (8) and for the presence or loss of the cDNA by polymerase chain reaction (PCR) amplification of genomic DNA (Fig. 2A). Those clones from which the cDNA was excised were all susceptible to infection, whereas the clones that retained the cDNA were resistant. These experiments confirmed that the cDNA was necessary for the virus resistance of the L1D3 line.

The cDNA insert in L1D3 was recovered from the genomic DNA by PCR amplification and cloned (8). To confirm that the cDNA was sufficient to induce virus resistance, the cDNA was recombined into the pBabe-HAZ vector and reintroduced into naïve Rat2 cells. Cells expressing the cDNA were again 30 times more resistant to the Eco-Luc virus than were the parental cells or cells carrying the empty vector (Fig. 2B). Thus, the expression of the cDNA was sufficient to establish viral resistance. To test whether the gene was only active against retroviral vectors or was also active against Moloney MuLV, we compared the kinetics of replication of wild-type MuLV in cells expressing the cDNA or the vector. Cells expressing the cDNA were resistant to virus replication, with a dramatic reduction in the level of production of progeny virus (Fig. 2C), although some virus eventually appeared at later times. At a very high multiplicity of infection, the resistance could be overcome, suggesting that the block to virus replication was not absolute.

The DNA sequence of the insert revealed a single open reading frame (ORF) of 254 codons fused to the zeocin resistance gene at its 3' end (Fig. 3A). The insert contained a long 5' untranslated region (UTR), and the ORF was not fused to HA at the 5' end; translation of the protein began at an AUG codon at the start of the ORF. Searches of the nucleic acid databases revealed two mouse expressed sequence tag (EST) clones with highly similar sequences [mEST995 and mEST896 (Fig. 3B)] differing only at their extreme 3' ends, a difference that probably arose through alternative splicing. Analysis of the available mouse genomic sequences identified a single gene encoding these mRNAs on chromosome 6. The sequence of mEST995 was used to design PCR primers, and the full-length sequence of the rat cDNA

was amplified and cloned (8). The complete cDNA contained 776 codons (deposited in GenBank, accession number AF521008); the

initial cDNA corresponded perfectly to the amino-terminal one-third of the sequence. The predicted amino acid sequences of the rat

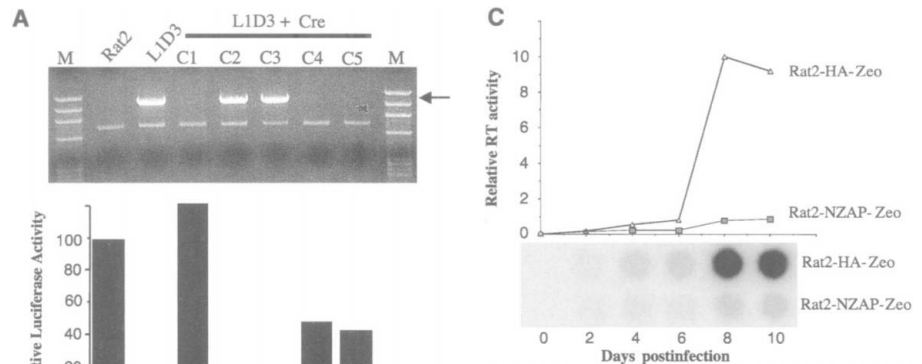
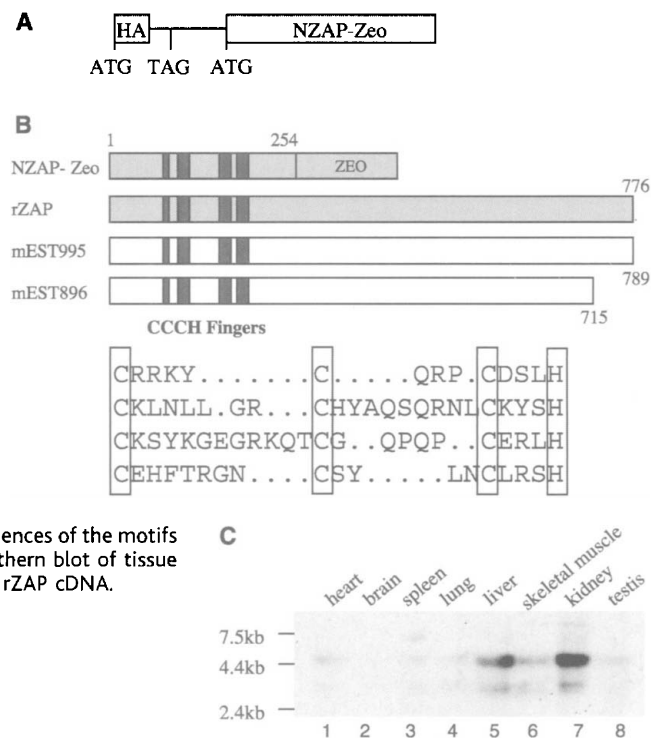


Fig. 2. Resistance of NZAP-zeo-expressing cells to virus infection. (A) Cre recombinase was stably introduced into L1D3 cells by cotransformation with pGK-puro. Five puromycin-resistant clones (C1 to C5) were expanded and tested for resistance to Eco-Luc virus (lower panel). Deletion of NZAP-zeo DNA was monitored by PCR (upper panel). M, marker DNAs; arrow indicates the position of the PCR-amplified DNA diagnostic of NZAP-zeo. (B) The NZAP-zeo fragment was recovered and reintroduced into naïve Rat2 cells and tested for resistance to Eco-Luc virus. Rat2, wild-type Rat2 cells; L1D3, L1D3 cells isolated from the screening; Rat2-HAZ, Rat2 cells expressing pBabe-HAZ vector; Rat2-NZAP-zeo, Rat2 cells expressing recovered pBabe-NZAP-zeo. (C) Cells were infected with wild-type MuLV at low multiplicity. The culture supernatants were harvested 2, 4, 6, 8, and 10 days after infection and were analyzed for reverse transcriptase (RT) activity to measure the spread of the virus. RT signals were quantitated by Phosphorimager and plotted.

Fig. 3. (A) Schematic representation of the cDNA fragment recovered from L1D3 cells. ATG, start codon; TAG, stop codon in 5' UTR; NZAP-zeo, ORF of NZAP-Zeo fusion. (B) A Blast search of the GenBank database with an NZAP fragment identified two mouse EST clones (mEST995 and mEST896) with high sequence similarity to rZAP. The 3' sequence of mEST995 was used to design a primer to PCR amplify full-length rZAP from a Rat2 cDNA library. Deduced amino acid sequences are compared. The four CCCH finger motifs are indicated by black boxes, and the sequences of the motifs in rZAP are shown. (C) Northern blot of tissue mRNAs of rat, probed with rZAP cDNA.



REPORTS

protein and of the similar mouse proteins contained a cluster of four potential, unusual, CCCH-type zinc fingers, previously found in only a few RNA binding proteins (Fig. 3B). Other than the conserved residues of the fingers, there was little sequence similarity to known proteins. The gene was named *rZAP*, for *rat Zinc-finger Antiviral Protein*, and the initial antiviral NH₂-terminal fusion construct was named NZAP-zeo.

To survey the expression of *rZAP*, we performed Northern blot analyses (Fig. 3C). The ZAP mRNA was present at high levels in the kidney and liver but was undetectable in the brain and testes. Two mRNAs (3.5 and 4.5 kb) were observed in most tissues, possibly corresponding to the two alternatively spliced mouse mRNAs in the database. Analysis of RNA from Rat2 cells revealed that *rZAP* mRNA was present at undetectably low levels (11), consistent with the high susceptibility of these cells to infection.

The resistance to virus transduction could potentially target many stages of infection. To determine the step in the retrovirus life cycle that was blocked, Rat2 cells expressing NZAP-zeo or the vector control were acutely infected with Eco-Luc virus,

and the synthesis of viral DNA was examined by PCR. Comparable levels of minus-strand strong-stop DNA were synthesized in both lines, suggesting that entry and initiation of reverse transcription were not inhibited (Fig. 4A). Similar experiments showed no defects in plus-strand DNA synthesis (11). To test for nuclear entry of the viral DNA, cells were infected with the vector Eco-green fluorescent protein (Eco-GFP), and circular viral DNAs were analyzed by PCR amplification of the LTR-LTR junction. Comparable levels of the circular forms were detected (Fig. 4A), suggesting no block to nuclear entry. To test for defects in viral gene expression, the retroviral Luc reporter DNA genome was introduced into cells by lipid-mediated transformation, bypassing the early stages of infection. The cells expressing NZAP-zeo expressed 30 times less luciferase than the controls, which was the same decrease seen after gene transfer by retroviral infection (Fig. 4B), suggesting that NZAP-zeo does not affect early events but rather inhibits retroviral gene expression. Expression of several control reporter genes lacking viral sequences was only reduced two- to threefold in the NZAP-zeo line (Fig.

4B), suggesting that MuLV genomes are specifically targeted by *rZAP*.

To examine the mechanism of the block of virus gene expression further, we measured viral mRNA levels in cells expressing NZAP-zeo or the empty vector. After infection with Eco-Luc virus, total cellular RNAs and fractionated nuclear and cytoplasmic RNAs (8) were examined for luciferase sequences by Northern blot (Fig. 4C). The whole-cell RNA preparations showed a modest reduction in the level of viral RNA in the NZAP-zeo cells as compared to the controls. The levels of the viral RNA in the nuclear fraction were virtually identical in the NZAP-zeo and control lines, suggesting that transcription initiation and elongation were not affected. The cytoplasmic viral RNA, however, was almost completely abolished in the NZAP-zeo cells, whereas high levels were found in the controls. Quantitation of longer exposures indicated that there was 30 times less cytoplasmic viral RNA in the NZAP-zeo cells than in the controls (Fig. 4C). The levels of rRNA, the housekeeping mRNA glyceraldehyde phosphate dehydrogenase (GAPDH) (Fig. 4C), and actin mRNA (12) were all unaffected. These results suggest that the

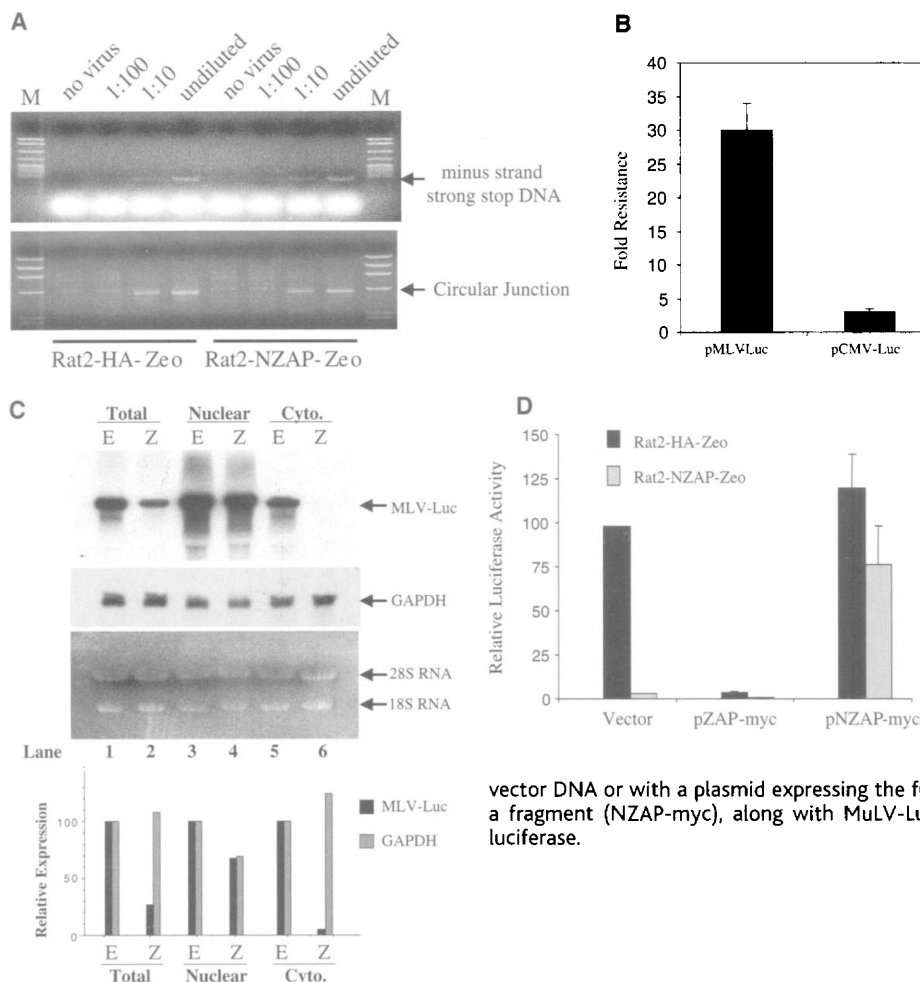


Fig. 4. Analysis of the block of virus infection. (A) Cells were infected with Eco-Luc (upper panel) or Eco-GFP virus (lower panel) at various dilutions. Viral DNA was extracted 24 hours after infection and detected by PCR using primers that amplify minus-strand strong-stop DNA or LTR-LTR circular junctions. (B) Cells were transiently transfected with DNA of the MuLV viral vector expressing luciferase (MLV-Luc) or with control vectors expressing luciferase (CMV-Luc and pGL3-Luc). After 48 hours, cells were lysed and luciferase activity was measured. (C) Cells were infected with undiluted Eco-Luc virus, and 48 hours later, total RNAs, nuclear RNAs, and cytoplasmic RNAs were isolated. The Eco-Luc RNAs were detected by Northern blot (top panel). The same membrane was stripped and reprobed with ³²P-labeled GAPDH DNA (middle panel). RNA levels were quantitated by Phosphorimager and plotted. RNAs in the gel were stained with ethidium bromide before transfer (bottom panel). E, Rat2-empty vector control cells; Z, Rat2-NZAP-zeo cells. (D) Rat2 cells stably expressing the vector (black bars) or NZAP-zeo (gray bars) were transiently transfected with

vector DNA or with a plasmid expressing the full-length ZAP (pZAP-myc) or a plasmid expressing a fragment (NZAP-myc), along with MuLV-Luc DNA. After 48 hours, lysates were assayed for luciferase.

NZAP-zeo protein specifically eliminated the cytoplasmic fraction of the viral RNA, with no effect on other cellular mRNAs.

The antiviral construct as originally isolated contained only the 5' one-third of the rZAP coding region, fused to the zeocin resistance gene. To test the function of the full-length protein, the complete ZAP ORF was cloned into an expression plasmid and tagged with a myc epitope at the carboxy terminus, forming pZAP-myc. pZAP-myc was used to transform Rat2 cells, and the effects on Eco-Luc transduction were measured as before. The full-length protein induced a dramatic inhibition of viral vector expression (Fig. 4D). The inhibition was even greater when rZAP and NZAP-zeo were expressed together. These results suggest that the full-length rZAP also acts to negatively regulate viral transcripts.

We tested other constructs to look for forms of ZAP that interfere with the antiviral activity of the wild-type protein. The 5' portion of the gene present in NZAP-zeo was excised from the pBabe-HAZ vector and expressed with a small myc epitope tag substituted for the zeo fusion partner (8). Surprisingly, the NZAP-myc fusion protein reproducibly caused a small increase, rather than a decrease, in the level of luciferase detected after cotransfection with Eco-Luc viral DNA (Fig. 4D). Moreover, this construct almost completely suppressed the inhibition in cells containing NZAP-zeo, restoring normal luciferase expression. Thus, this fragment antagonized the normal rZAP activity. This distinct and opposite behavior of NZAP-myc from NZAP-zeo presumably reflects differences in the size or structure of the fusion partners in these two constructs.

These results show that direct selections for virus-resistant cells (9) can be used to identify new genes with potent antiviral activity. The gene recovered here, rZAP, is sufficient to induce an antiviral state with no apparent effect on cell viability or physiology. ZAP profoundly inhibits the expression of genes carried by retroviral vectors, at the level of the cytoplasmic viral RNA. The presence of four unusual CCCH-type zinc fingers suggests that ZAP interacts directly with the viral RNA. These fingers are found in a small family of RNA binding proteins that includes tristetraprolin (TTP), which negatively regulates the levels of tumor necrosis factor- α (TNF- α) (13), and granulocyte-macrophage colony-stimulating factor mRNAs (14). TTP binds AU-rich sequences in the 3' UTR of the TNF- α mRNA (13, 15) and recruits the exosome to degrade the mRNA (16). rZAP may act in a similar way at sequences found in viral RNAs.

The normal function of rZAP may be to regulate one or more specific cellular mRNAs. However, like PKR, RNase L, and the Mx proteins, rZAP may primarily func-

tion to inhibit viral gene expression and induce an innate immunity to viral infection. The full range of viruses restricted by rZAP is not yet known; however, rZAP potently blocks replication of Sindbis virus in Rat2 cells (17). Activation of expression of the endogenous gene could help induce immunity and protect individuals from disease caused by viral infections.

References and Notes

1. D. E. Levy, A. Garcia-Sastre, *Cytokine Growth Factor Rev.* **12**, 143 (2001).
2. S. Landolfo, G. Gribaudo, A. Angeretti, M. Gariglio, *Pharmacol. Ther.* **65**, 415 (1995).
3. S. D. Der, Y. L. Yang, C. Weissmann, B. R. Williams, *Proc. Natl. Acad. Sci. U.S.A.* **94**, 3279 (1997); B. R. Williams, *Oncogene* **18**, 6112 (1999).
4. O. Haller, M. Frese, G. Kochs, *Rev. Sci. Tech.* **17**, 220 (1998); M. Frese, G. Kochs, H. Feldmann, C. Hertkorn, O. Haller, *J. Virol.* **70**, 915 (1996); J. Pavlovic et al., *J. Virol.* **69**, 4506 (1995).
5. M. R. Player, P. F. Torrence, *Pharmacol. Ther.* **78**, 55 (1998).
6. I. M. Kerr, R. E. Brown, *Proc. Natl. Acad. Sci. U.S.A.* **75**, 256 (1978).
7. A. Zhou, J. M. Paranjape, S. D. Der, B. R. Williams, R. H. Silverman, *Virology* **258**, 435 (1999).

8. See supporting online material for details.
9. G. Gao, S. P. Goff, *Mol. Biol. Cell* **10**, 1705 (1999).
10. pMC-Cre, expressing the Cre recombinase [G. W. Bothe, J. A. Haspel, C. L. Smith, H. H. Wiener, S. J. Burden, *Genesis* **26**, 165 (2000)] was a generous gift from S. J. Burden, New York University.
11. G. Gao, X. Guo, S. P. Goff, unpublished observations.
12. _____, data not shown.
13. W. S. Lai et al., *Mol. Cell. Biol.* **19**, 4311 (1999).
14. E. Carballo, W. S. Lai, P. J. Blackshear, *Blood* **95**, 1891 (2000).
15. W. S. Lai, P. J. Blackshear, *J. Biol. Chem.* **276**, 23144 (2001); W. S. Lai, E. Carballo, J. M. Thorn, E. A. Kennington, P. J. Blackshear, *J. Biol. Chem.* **275**, 17827 (2000).
16. C. Y. Chen et al., *Cell* **107**, 451 (2001).
17. M. MacDonald, personal communication.
18. Supported by Public Health Service grant CA 30488 from the National Cancer Institute. G.G. is a Special Fellow of the Leukemia and Lymphoma Society, and S.P.G. is an investigator at the Howard Hughes Medical Institute.

Supporting Online Material

www.sciencemag.org/cgi/content/full/297/5587/1703/DC1

Materials and Methods

Figs. S1 and S2

References

23 May 2002; accepted 29 July 2002

Spatiotemporal Pattern of Neural Processing in the Human Auditory Cortex

Erich Seifritz,^{1*} Fabrizio Esposito,² Franciszek Hennel,³ Henrietta Mustovic,¹ John G. Neuhoff,⁴ Deniz Bilecen,⁵ Giocchino Tedeschi,² Klaus Scheffler,⁶ Francesco Di Salle⁷

The principles that the auditory cortex uses to decipher a stream of acoustic information have remained elusive. Neural responses in the animal auditory cortex can be broadly classified into transient and sustained activity. We examined the existence of similar principles in the human brain. Sound-evoked, blood oxygen level-dependent signal response was decomposed temporally into independent transient and sustained constituents, which predominated in different portions—core and belt—of the auditory cortex. Converging with unit recordings, our data suggest that this spatiotemporal pattern in the auditory cortex may represent a fundamental principle of analyzing sound information.

One of the basic operations that the auditory system performs to decode acoustic information is the temporal analysis of sound features and their decomposition into specific neural dis-

charge patterns. The importance of temporal analysis in audition is evident considering that the sensory stream emerges mainly in series over time. Decomposition and integration in the time domain are used for the qualitative and quantitative perceptual analysis of sound information (1, 2), and neural mechanisms specifically dealing with temporal pattern analysis are essential for the processing of complex auditory signals. In animals, neurons of the auditory cortex can be broadly classified into transient and sustained responders. Transient responses typically occur at the onset of a stimulus, whereas sustained responses follow the stimulus (3–9). In the human auditory cortex, the spatiotemporal principles of encoding sound information are not yet fully understood. Magnetoencephalography demonstrated transient and steady-state re-

¹Department of Psychiatry, University of Basel, 4025 Basel, Switzerland. ²Second Division of Neurology, Second University of Naples, 80138 Naples, Italy. ³Magnetic Resonance Department, 44691, Fondation pour la Recherche Appliquée en Psychiatrie, Hospital Center, 68250 Rouffach, France. ⁴Department of Psychology, The College of Wooster, Wooster, OH 44691, USA. ⁵Department of Radiology, University of Basel, 4031 Basel, Switzerland. ⁶Section for Medical Physics, Department of Radiology, University of Freiburg, 79106 Freiburg, Germany. ⁷Department of Neurological Sciences, Division of Neuroradiology, University of Naples Federico II, 80127 Naples, Italy.

*To whom correspondence should be addressed. E-mail: erich.seifritz@unibas.ch